[논 문] 한국재료학회지
Korean Journal of Materials Research
Vol. 7, No. 3 (1997)

LASER CONSOLIDATION OF THE PLASMA COATED CHROME CARBIDE LAYER

안 희 석 · 이 창 희

레이저를 이용한 크롬카바이드 플라즈마 용사층의 특성향상

Hee Seok An and Chang Hee Lee

(Dept. of Met. Eng., Research Institute of Steel Process and Application, Hanyang University, 17 Haengdang-Dong, Seongdong-Ku, Seoul 133-791)

(1996년 12월 13일 받음, 1997년 1월 24일 최종수정본 받음)

Abstract This paper evaluated the feasibility of laser consolidation for improving the properties of the plasma coated layer. Further, the mechanim of the degradation sequence of the chrome carbide layer applied on the turbine blades was postulated.

The laser consolidation could be successfully applied for improving the surface properties of the plasma coated blade, if a proper condition was carefully chosen. The consolidated layer had erosion & corrosion resistance and bond strength superior to those of the as-plasma coated layer. The properties of the consolidated layer were strongly dependent upon the degree of dilution, especially on the Fe pickup from the substrate.

The degradation of the plasma coating layer was thought to be a result of the repeating action of the solid particle erosion, corrosion penetration through the pores and oxide films formed along the interlayer surface and impact spalling.

1. Introduction

The blades in the Top-over gas Reduction Turbine (TRT), which is running by the blast furnace gas(BFG : mixture of CO_2, CO, H_2, H_2S and N_2) in the iron & steel making mill, are significantly impaired by erosion and corrosion. Although the BFG is cleaned and cooled (to about 50℃) by passing through both dry and wet type dust catchers before flowing into the turbine, it normally includes a small amount of dust(5mg/m^3) and mist(mixture of dust and moisture, 10 g/m^3), which may be sufficient enough to damage blades under the flowing speed of about 35m/min[1]. Therefore, the chrome carbide type protective coating which is known to have a good corrosion and erosion resistance to the turbine environment was applied on the blade surface by the high power plasma spraying process. Though the applied coating served very well for a short period of operation, it was eventually peeled off by the inpacting action of the residual dust and mist, and thus it did not noticeably improve the campaign life of the blades. A typical edge debonding of the plasma coated layer is shown in Fig. 1.

Therefore, this study evaluated the feasibility of the laser consolidation process in improving the properties of the thermal sprayed chrome carbide coating such as erosion resistance, corrosion resistance, bond strength, and amount of pores. The properties of the laser treated layer was correlated with microstructures and chemistries. Further, the degradation sequence of the plasma coating layer was also postulated.

2. Material and Experimental Procedures.

2.1 Materials

The chemical composition of the substrate utilized is given in Table 1. It was melted and forged(Finishing temp. 950℃) in the laboratory in order to get the microstructure equivalent to that of the actual blade. Powder for the plasma spraying was 75%Cr_3C_2+25%NiCr(sintered and crushed) with the size range of 5-45μm, The plasma spraying condition was that suggested by the supplier and is given in Table 2. The thickness of the plasma coating layer was about 300μm.

2.2 Experimental Procedures

The laser was a continuous wave type CO_2 with the maximum power of 3kW. For the surface consolidation, the laser beam was defocused with ZnSe lens to give 3mm dia at the surface of the substrate and the scan

Table 1. Chemical composition of the substrate

Type	C	Si	Mn	P	S	Ni	Cr	Mo	V
AISI 403	0.128	1.511	0.923	0.022	0.066	0.677	13.10	0.607	0.059

Table 2. Approximate chemistry of the laser consolidated surface(EPMA)

Scan Rate	Composition				
	Fe	C	Cr	Ni	Si+Ca+Mg+Co
81VF As coated	--	9.80	71.88	16.99	1.306
1000	73.27	1.63	21.32	3.33	0.45
1600	65.69	1.89	26.66	5.55	0.21
1900	61.85	2.30	29.29	6.03	0.55
2600	52.94	3.34	35.82	7.34	0.56
3400	42.70	5.17	43.20	8.33	0.60
4400		10.06	70.64	16.16	1.14

Fig. 1. A typical appearance of the debonded plasma coating.

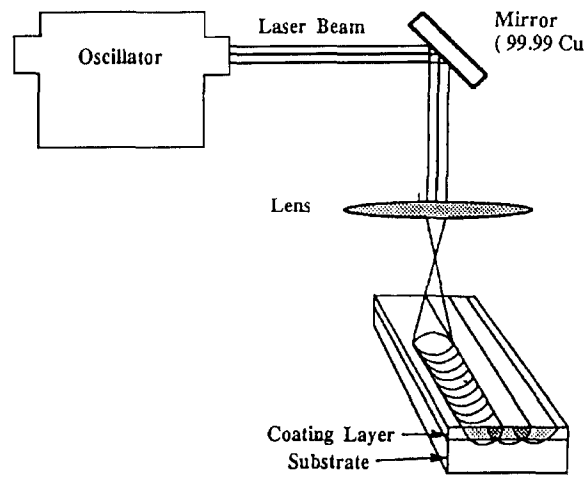

Parameter	Condition
Laser	CO_2
Beam Size	3 mmø
Power	2.1 kW
Scan Rate	1000, 1600, 1900, 2600, 3400, 4400 mm/min

Fit. 2. Approximate chemistry of the laser consolidated surface (EPMA)

rate was varied from 1000mm/min to 4400 mm/min under the constant beam power of 2.4kW. Ar assist gas was blown throughout the operation to protect the melt pool from the possible contamination. A schematic representation of the laser consolidation setup is shown in Fig. 2.

The erosion properties of the plasma coating layer and the laser consolidated layer were evaluated by the solid particle impact erosion test. The test conditions were; powder-200 mesh Al_2O_3, velocity-40m/sec, impact angle-30°, temperature-ambient, and other de-

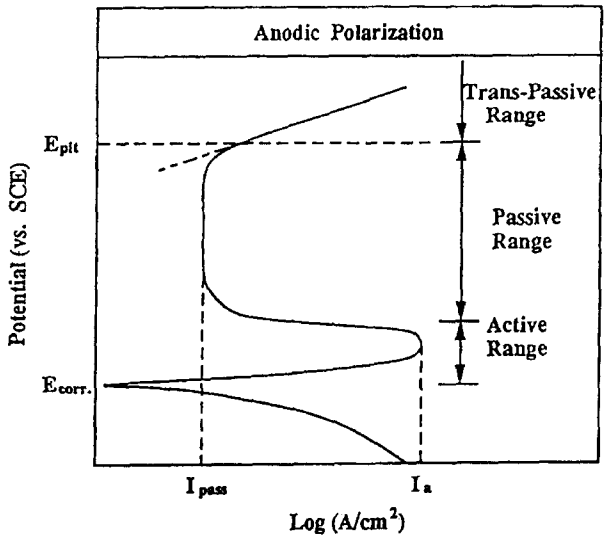

Parameter	Condition
Solution	1N H_2SO_4 + 3.5% NaCl
Temperature	Room Temperature
Scan Rate	1 mV/sec
Surface Finish	#600 Paper
Reference Electrode	Hg - HgCl (SCE)
Deaeration	None

Fig. 3. A schematic representation of the anodic polarization technique and test conditions.

tails which are given in ref[2-4].

The corrosion resistance was measured by the anodic polarization technique in the $1NH_2SO_4-3.5NaCl$, and the definitions of important points and test conditions are given in Fig. 3. Further, some selected samples were also immersion tested in the same solution as that for the polarization technique for one month in order to investigate any effects of the discontinuities such as porosity and oxides along the interlayer surface on the corrosion penetration and bond strength. Edge and substrate were enveloped with epoxy resin before the immersion test to ensure that only the plasma coating surface would be exposed to the solution.

Bond strength was measured according to ASTM 633[5]. Area fraction of pores was estimated from the metallographic samples by the image analyzer. Eight out of the ten random measurements excepting the highest and lowest values were used for the calculation of average pore density. Vicker's microhardmess was measured under the constant load of 500g. Microstructural characteristics of the plasma coating and laser consolidated layers were evaluated by using OLM, SEM (EPMA), TEM and XRD.

3. Results and Discussion

3.1 Degradaton of the Plasma Coating Layer

Microstructure and bond strength

A typical microstructure with a Cr, Ni distribution in the thickness direction of the as plasma coated layer is shown in Fig. 4. The coating appears to have repetitive layers of dark and bright features. While Cr is enriched in the dark region, the bright region is enriched with Ni, revealing that the dark and bright regions were from the chrome carbides and NiCr self-flux, respectively.

Microstructure also reveals significant of pores formed along the interlayer region(see P). The measured area fraction of the pores was about 5.5%. Imperfections or misbondings can also be found along the coating-substrate interface(see arrows), which can reduce the bond strength significantly. The measured bond strength was varied from 4.6 to 8kg/mm^2 depending upon the amount of the imperfections along the interface in the sample, and the average strength was 5.8

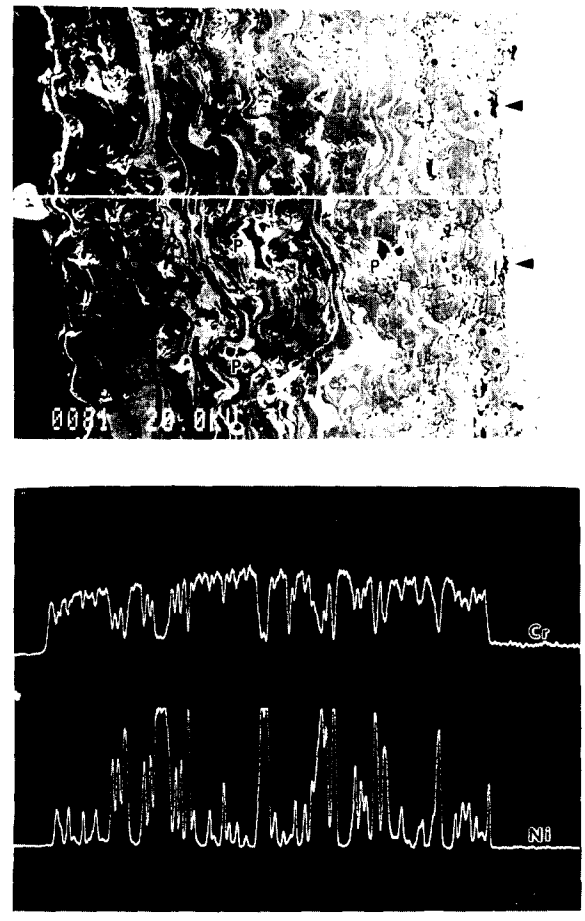

Fig. 4. Typical cross sectional view of the plasma coating and Cr, Ni distriburtion

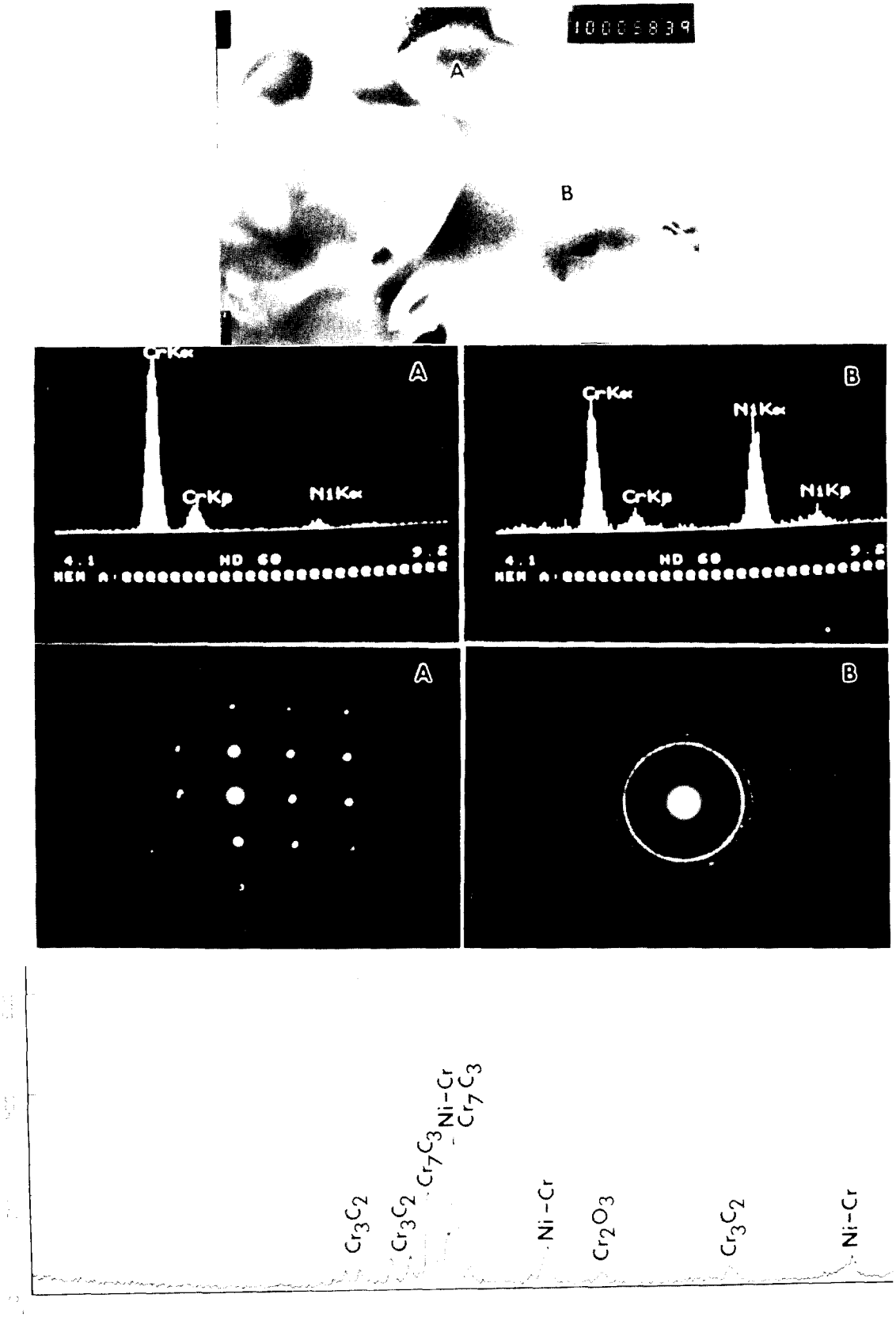

Fig. 5. Microstructure, SAD and XRD from the non-treated plasma coating

kg/mm². Further, some of the incompletely melted powders and oxide films in the interlayer can also be noticeable.

TEM microstructure and SAD from the plasma coat-

ing, as given in Fig. 5, show some of the unmelted Cr_3C_2 and glassy NiCr strudtures. The glassy structure, which was unexpectable, was found only in the outer surface region of the coating. In the other regions near the interface, the originally formed glassy structure mny have transformed to the crystal struture by the heat of the subsequent layers. Further, transformation of the Cr_3C_2 to Cr_7C_3 during solidification and cooling can also be noticed from XRD in the bottom of Fig. 5.

Corrosion and Erosion

The corrosion resistance of the plasma coating, measurd by the anodic polarization technique as shown in Fig. 6, is superior to that of the surbstrate and almost-equivalent to that of the laser consolidated layer which was not diluted with the substrate. However, when the scan rate was slow enough that the layer was diluted with substrate, different corrosion behavior was found dna it will be further discussed in a later section.

The pores and other discontinuities in the coating did not seem to exert detrimental influence on the corrosion resistance in the test. This may be due to a relatively short time exposure to the corrosive environment in the polarization test. Therefore, some selected samples were dipped in the 1N H_2SO_4+3.5% NaCl solution for one month, and then the surface and corss-section were carefully examined to see if any corrosion damage had occurred. There was no detectable corrosion damage on the surface. However, as shown in Fig. 7, a severe corrosion penetration into the interlayer boundaries, which was found to be decorated by the pores and oxide films, and into the coating-substrate interfaec can be found from the cross-section. The corrosion penetration into the interlayer and interface may have played a critical role in debonding of the plasma coating layer during the operation of a turbine blade. A similar corrosion penetration in the plasma coating was also

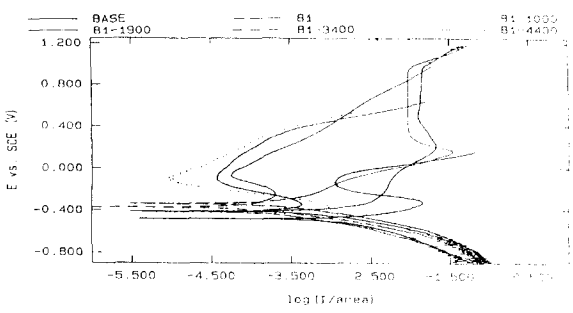

Fig. 6. Anodic polarization behavior of substrate, plasma coating and laser treated layers.

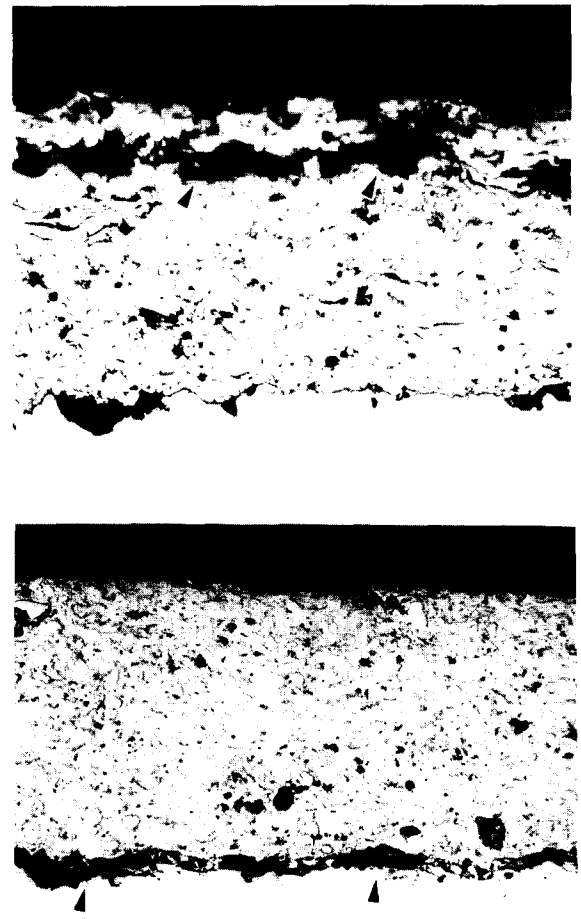

Fig. 7. Corrosion penetration through pores/discontinuties into the interlayer(a) and the interface between substrate and coating(b).

found by other investigators.[7,8] Onece the corrosion penetration has occurred along the interlayer, impacting dust and mist particles can easily spall the layer off. The measured bond strenth after a corrosion test was as low as 1.2kg/㎟ which is significantly lower than that of the as-coated condition.

Fig. 8 shows a microscopic appearance of the plasma coating surface after an erosion test. Erosion appears to occur with a deformation mechanism typical in the ductile materials such that impacting particles generate ditches with shear lips around the edge, and then subsequent impacts deform the lips and thus eventually detach those from the surface. The smooth appearance of the localized surface indicates that some of the layers may be spalled off along the interlayer boundaries which were decorated by the oxide films and pores.

Proposed degradation sequence

Based on the above results of corrosion and erosion tests, premature failure of the plasma coating in the TRT blade may be the result of the repeating action of

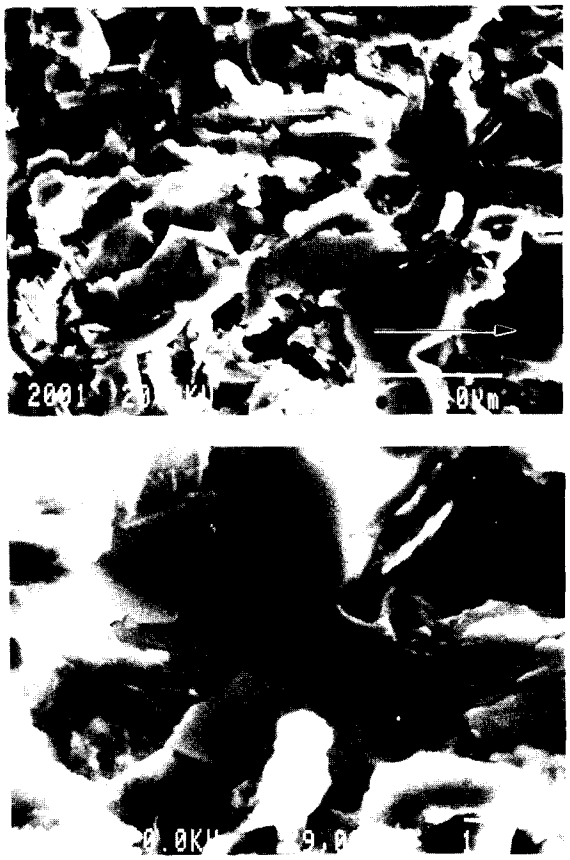

Fig. 8. Appeatance of the plasma coating surface after particle erosion test

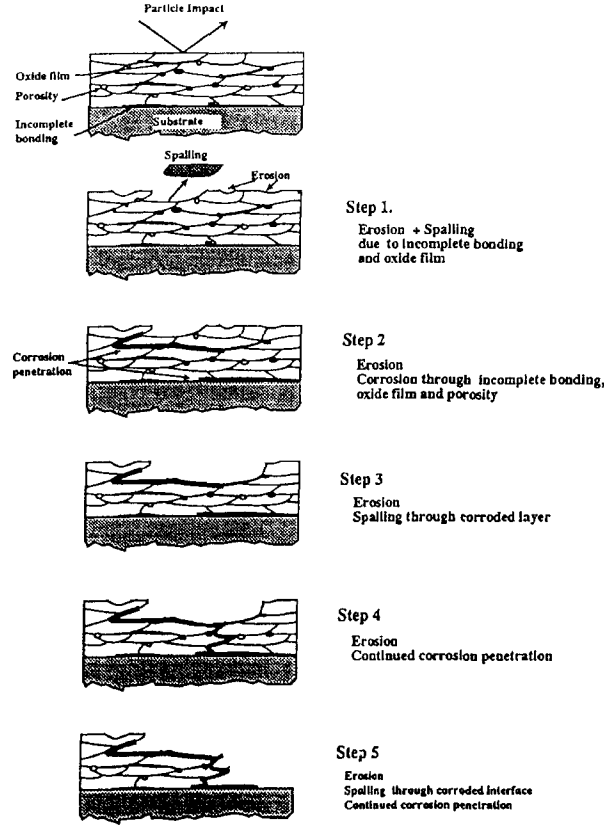

Fig. 9. A postulated degradation sequence of the plasma coating.

solid particle erosion, corrosion penetration and impact spalling. A proposed degradation sequence of the plasma coating is schematically shown in Fig. 9. Before the corrosion penetration decreases the interlayer bond strength, impacting particles erode the surface and detach some layers whose interboundaries are decorated with oxide films and pores, resulting in a low interlayer cohesive strength which will result in an accelerated spalling of the layers by the subsequent impacting particles. These repetitive actions of the erosion, corrosion penetration and spalling proceeds until the bare substate is exposed to the severe erosive and corrosive environment. Therefore the plasma coating itself does not noticeably improve the campaign life of the blade in the currently considered environment.

Therefore, a possible way of extending the campaign life of the plasma coating is the reduction of the pores and oxides either by the careful control of the process parameter or by the consolidating(remelting and densification) of the coating. In the following section, the microstructural characteristics and properties of the laser consolidated layer are discussed.

3.2 Laser consolidation

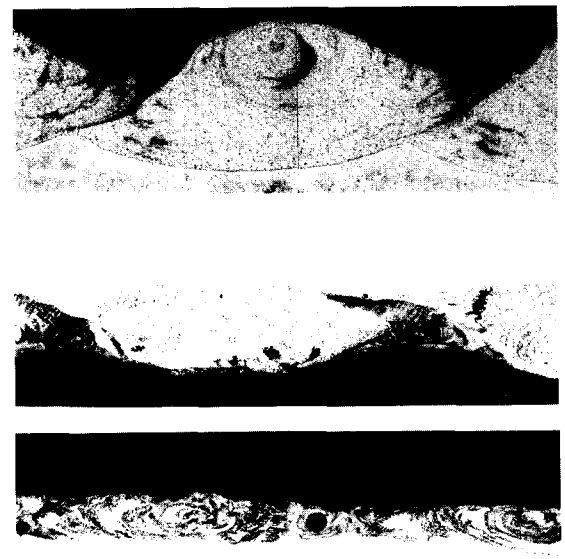

Fig. 10. Macroscopic appearaned of the laser consolidated layer as a function of rate(1000, 1900, 3400 ㎜/min).

Microstructural characteristics

Fig. 10 shows a typical macroscopic appearance of the cross-sections of the laser consolidated layer as a function of the scan rates(1000, 1900, 3400㎜/min).

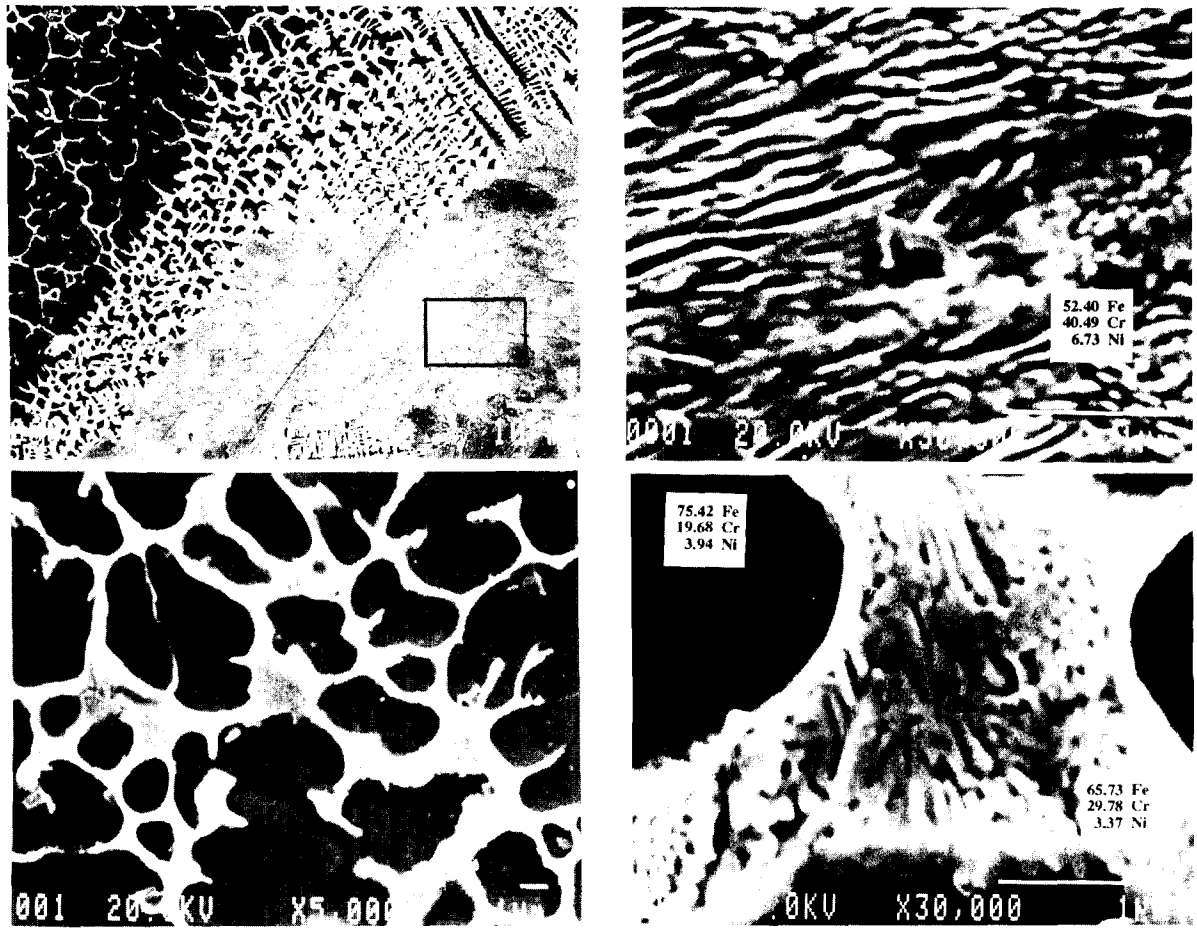

Fig. 11. Magnified microstructures near the overlapped region.

As it may be expected, the size of the melted region decreases by increasing the scan rate. Further, as the scan rate is raised, an amount of the darkly appearing structure increases, especially in the overlapped region. A magnified microstructires of the white and dark region are given in Fig. 11 with approximate chemistries (SEM/EPMA).While the white region has a microstructure similar to the 304 stainless weld metal, the dark region has a feather like morphology. The dendrite boundary in the white region has higher Cr content with lower Fe and Ni than that in the dendrite core. The feathery microstructure has the highest Cr Content and the lowest Fe content. Although each type of the structures could not be easily indentified, the dendrite boundary and feathery region could be a mixture of C saturated Fe-Cr-Ni and M_7C_3 predicted from the XRD (Fig. 12) and the Fe-Cr-C ternary diagram[7]. As the scan rate decreases the dilution from the substrate increases(i.e, increase Fe pick-up, see Table 2), and thus the amount of C saturated Fe-Cr-Ni increases while amount of M_7C_3 decreases as shown in XRD).

Porosity

The variation of the porosity density in the laser consolidated layer as a function of the scan rate is given in Fig. 13a. There is very little porosity in the layer until the scan rate approaches to about 4000m/min. However, when the scan rate becomes 4400 ㎜/min, the fastest speed evaluated in this study, the amount of pores abruptly increases to about 9%, which is greater than that in the plasma coating.

The cross-section of the layer, scaned with 4400㎜/min, is shown in Fig. 13b. With this speed, only half thickness of the coating was remelted and thus there was no dilution with plasma coating and cracks appear to initiate from the large pores. The abrupt increase in the porosity is believed to be due to the agglomeration of the exixting small pores in the plasma coating. Once pores agglomerate, these are entrapped in the melted region because of the rapid solidification rate. Therefore, the scan rate should be carefully controlled to ensure some amount of a dilution with the substrate.

Bond strength and Hardness

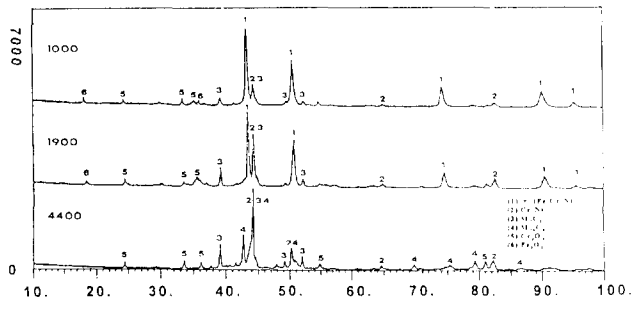

Fig. 12. XRD results from the laser treated surfaces.

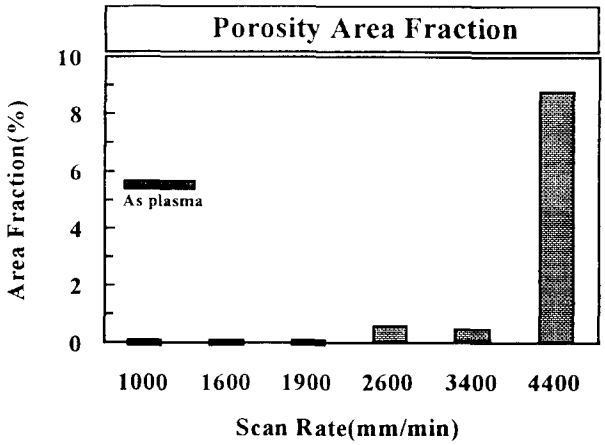

(a)

(b)

Fig. 13. Variation of the areal fraction of pores as a function of scan rate(a) and cross section appearance of a layer(4400㎜/min)(b)

The bond strength variation in the consolidated layer is shown in Fig. 14a as a function of the scan rate. As it may be expected from the microstructures, the strength of the consolidated layer is as high as 10kg/㎟ as long as the original defective plasma coating-substrate interface was remelted and formed no detectable discontinuities along the new interface. However, if the scan rate is so fast that no dilution occurs, the bond strength significantly drops to the lower value than that of the original plasma coating. Therefore, it emphasizes, here again, the importance of the scan rate control.

Hardness variation with the scan rate is given in Fig. 14b. The hardness of the consolidated layer increases with an increase in the scan rate. Hardness variation can be explained with the C content, i.e., as the scan rate increases the dilution with the substrate decreases and thus the carbon in the layer increases(Table 2). Therefore, the faster the scan rate is, the more carbide (M_7C_3) forms as shown in XRD(Fig. 12) and thus the higher the hardness is. Further, a finer structure with the faster scan rate may have also been played.

Erosion

Fig. 15 compares the erosion resistance of the substrate, plasma coating and laser consolidated layer. The hatched and spotted bars represent the average erosion loss of the substrate and the plasma coating respectively. The laser consolidated layer, regardless of the scan rate, has a greater erosion resistance as compared to those of the substrate and the plasma coating.

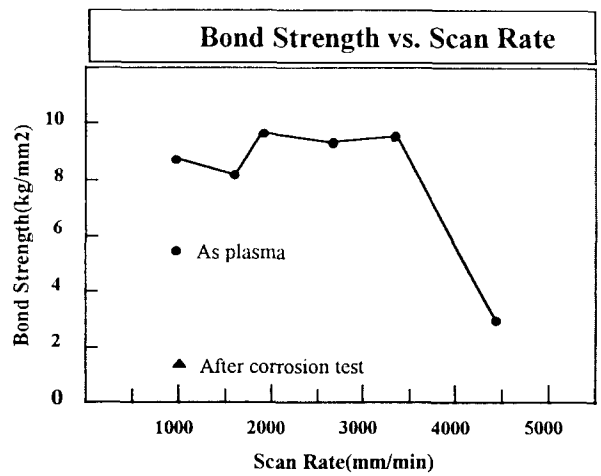

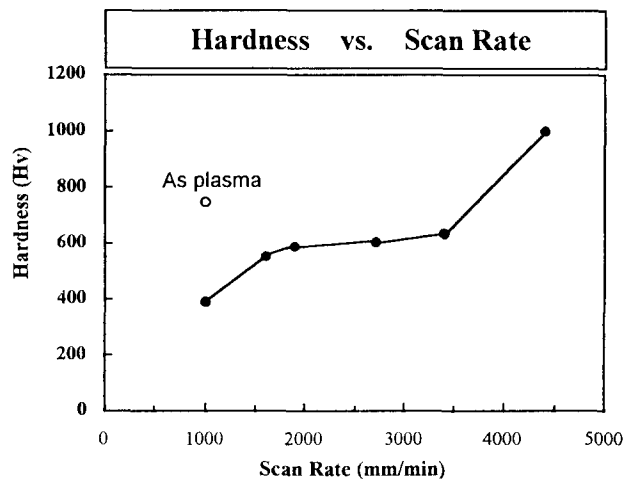

Fig. 14. Variations in bond strength and surface hardness as a function of laser scan rate.

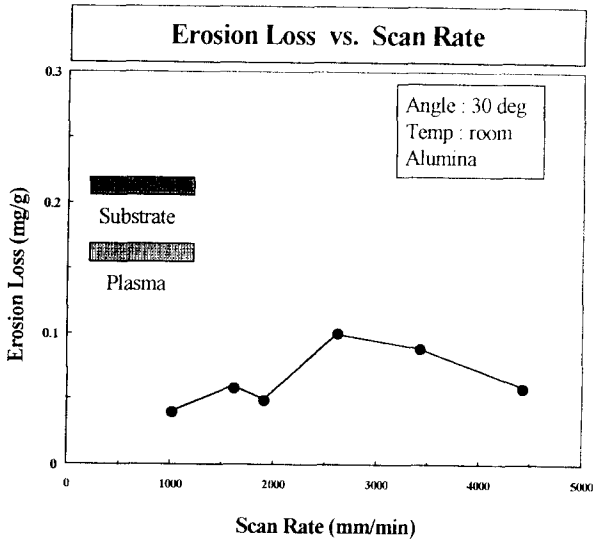

Fig. 15. Comparison of erosion loss among substrate, plasma coating and laser treated layers.

It should be noted that although the highest scan rate (4400㎜/sec) did generate a considerable amount of po rosity and cracks, the erosion loss did not increase in the current short time laboratory erosion test. However, a long time exposure in the actual environment should result in an increased erosion loss and corrosion loss.

When comparing with the hardness results in Fig. 14b, the erosion resistance of the materials is not a function of the surface hardness. There is no clear rela tionship between the hardness and the erosion loss, un like the case of wear properties.

Corrosion

The anodic polarization behavior of the laser consoli dated layers is compared with those of the substrate and the plasma coating in Fig. 6. It clearly shows that the laser remelted layer has a better general corrosion as compared to that of the substrate. Both the pitting potential and passivation range are greater than those of the substrate. A summary of the pitting potential and passivation potential range is given in Fig. 16.

Although the absolute pitting potential and passivation potential range of the plasma coating are greater than that of the laser consolidated layer, it can not be assumed that the corrosion resistance of the plas ma coating could be better than that of the laser consol idated layer, because the corrosion current density in the passivation range of the consolidated layer is con siderably smaller than that of the plasma coating. Therefore, byth the pitting and general corrosion are considered, the laser consolidated layer can perform better in the chloride containing sulfate solution.

Fig. 17 shows a typical macro-appearance of the

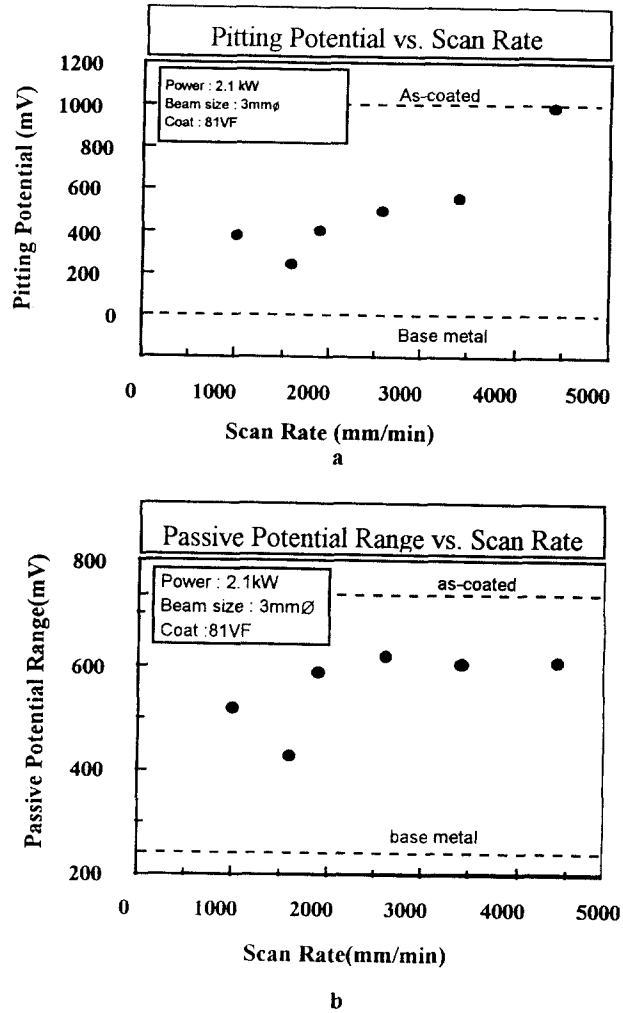

Fig. 16. Variation of pitting potential and passive potential rang as a function of laser scan rate.

laser treated layer after the anodic polarization test. Some selective attacks in the layer can be observed. The attack appears to occur at the whitely appearing region which had a higher Fe content as discussed earli er. Therefore the non-uniform microstructure in the laser consolidated layer can result in a localized corro sion problem and thus additional laser scan may be re quired for the uniform microstructure and for a better corrosion performance in the service.

4. Summary

From the above results and discussion, if a proper condition is chosen the state of the art technique-laser consolidation can be successfully applied for improving the properties of the plasma coated turbine blade. The following results can be drawn,

1) A possible sequence for the deterioration of the plasma coating during service was postulated. It was the result of the repeating actions of particle erosion, corrosion penetration through the interlinking pores and oxide films along the interlayer and impact spall

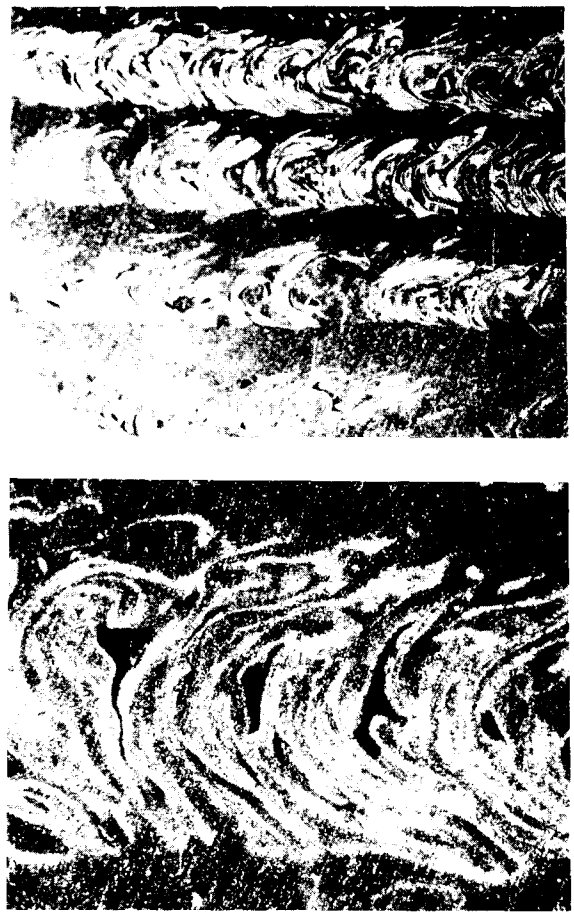

Fig. 17. Typical surface appearance of a highly diluted(Fe pick up) laser treated layer(1000㎜/min) after corrosion test.

ing.

2) The laser consolidation could enhance the erosion resistance, bond strengh and reduce the pore density as compared to the as-plasma coated condition. While the corrosion resistance was also improved, a localized attack due to the non-uniform microstructure in the laser consolidated layer may be troublesome.

3) For an optimum property, choice of the scan rate under the constant beam power and size was most critical, and it should be the speed which can ensure a small dilution with the substrate.

Acknowledgement

This study was partially supported by A 1995 NON-DIRCTED RESEARCH FUND, The Korea Research Foundation.

References

1. C.H. Lee, et.al. Improvenent of turbine life for fossil energy application. Technical Report RIST-10632A, 1992.
2 . J.B. Ju, et.al. A comparative study of the slurry erosion and free-fall particle erosion of aluminum. Wear of Materials, ASM, 1991, 416.
3. A.V. Levy, et.al. Erosion of hard material coating systems. ibid.
4. T. Singh, et.al. The erosion behavior of 304 stainless steel at elevated temperatures. Metallurgical Transactions, 21A, 1990, 3187.
5. ASTM C633. Standard test method for adhesion or cohesive strength of flame-sprayed coatings. ASTM, 1980, 654.
6. J.D. Ayers, et.al. Corrosion behavior of laser consolidated titanium coated steel in sea water. Corrosion, 37(1), 1981, 55.
7. H. Bgat, et.al. Laser processing of plasma-sprayed NiCr coatings. Conference Proceedings, Lasers In Materials Processing. Edited by E.A. Metzbower, ASM, 1984.
8. ASM Handbook Vol 3. Alloy phase diagram. ASM International, 1992.